Targeted disruption of the Cl^-/HCO_3^- exchanger Ae2 results in osteopetrosis in mice

Kaj Josephsen[a,b], Jeppe Praetorius[a,c], Sebastian Frische[a,c], Lara R. Gawenis[d], Tae-Hwan Kwon[e], Peter Agre[f,1], Søren Nielsen[a,c,1], and Ole Fejerskov[a,c]

[a]The Water and Salt Research Center, Faculty of Health Sciences, [b]Department of Dental Pathology, Operative Dentistry and Endodontics, School of Dentistry, and [c]Institute of Anatomy, University of Aarhus, DK-8000 Aarhus C, Denmark; [d]Department of Molecular Genetics, Biochemistry, and Microbiology, 231 Albert Sabin Way, ML524, University of Cincinnati College of Medicine, Cincinnati, OH 45267-0524; [e]Department of Biochemistry and Cell Biology, School of Medicine, Kyungpook National University, Taegu 700–422, Korea; and [f]Department of Molecular Microbiology and Immunology, Johns Hopkins Malaria Research Institute, Bloomberg School of Public Health, 615 North Wolfe Street, Baltimore, MD 21205

Contributed by Peter Agre, November 23, 2008 (sent for review September 6, 2008)

Osteoclasts are multinucleated bone-resorbing cells responsible for constant remodeling of bone tissue and for maintaining calcium homeostasis. The osteoclast creates an enclosed space, a lacuna, between their ruffled border membrane and the mineralized bone. They extrude H^+ and Cl^- into these lacunae by the combined action of vesicular H^+-ATPases and ClC-7 exchangers to dissolve the hydroxyapatite of bone matrix. Along with intracellular production of H^+ and HCO_3^- by carbonic anhydrase II, the H^+-ATPases and ClC-7 exchangers seems prerequisite for bone resorption, because genetic disruption of either of these proteins leads to osteopetrosis. We aimed to complete the molecular model for lacunar acidification, hypothesizing that a HCO_3^- extruding and Cl^- loading anion exchange protein (Ae) would be necessary to sustain bone resorption. The Ae proteins can provide both intracellular pH neutrality and serve as cellular entry mechanism for Cl^- during bone resorption. Immunohistochemistry revealed that Ae2 is exclusively expressed at the contra-lacunar plasma membrane domain of mouse osteoclast. Severe osteopetrosis was encountered in Ae2 knockout (Ae2−/−) mice where the skeletal development was impaired with a higher diffuse radio-density on x-ray examination and the bone marrow cavity was occupied by irregular bone speculae. Furthermore, osteoclasts in Ae2−/− mice were dramatically enlarged and fail to form the normal ruffled border facing the lacunae. Thus, Ae2 is likely to be an essential component of the bone resorption mechanism in osteoclasts.

anion exchanger | bone resorption | osteoclast

Human osteopetrosis has almost exclusively been associated with defects in acidification of the microenvironment of the resorptive lacunae (1), rather than a lack of proteolytic enzymes or transcytotic processes. The H^+-ATPase (2, 3) and ClC-7 (4) are established as directly responsible for translocating H^+ and Cl^- across the ruffled border to establish low pH (4.5–4.8 units) of the lacuna (5). Likewise, carbonic anhydrase isoenzyme II (CAII) has been shown to be necessary for intracellular generation of protons, H^+ (6). However, the mechanisms involved in contra-lacunar import of Cl^- to and extrusion of excess HCO_3^- from the osteoclast, which would be required for sustained resorptive function (7), remain elusive. Ae proteins of the Slc4A gene family are Cl^-/HCO_3^- exchangers and play a major role in the regulation of intracellular pH (pH_i), cell volume, migration, and to some degree, transepithelial ion movement in various tissues (8). Deficiencies of the expression of Ae proteins lead to very distinct phenotypes. Human SLC4A1 (AE1) mutations cause either the erythroid disorders "spherocytic hemolytic anemia" or "ovalocytosis", or distal renal tubular acidosis (9). Human SLC4A3 (AE3) polymorphisms have been associated with seizures (10). In contrast to AE1 and AE3, hereditary human diseases related to the AE2 gene have not been reported. Human AE2 mutations might be lethal because of the wide tissue expression pattern of the AE2, and because a severe phenotype was described for Slc4a2/Ae2 knockout mice that included growth retardation and death by the age of weaning (11). Ae2 is expressed in the choroid plexus, gastric parietal cells, throughout the GI tract, and in the respiratory and genital tracts (8). It is also expressed throughout the kidney tubule, most abundantly in the medullary thick ascending limb and the inner medullary collecting duct (12). Moreover, Ae2 mRNA has been found in osteoclasts (8), suggesting that Ae2 could play a role in Cl^-/HCO_3^- exchange by this tissue. In the present study, we aimed to complete the molecular model for lacunar acidification of ostecolast, hypothesizing that a HCO_3^- extruding and Cl^- loading anion exchange protein would be necessary to sustain bone resorption by osteoclasts. The results revealed that Ae2 is selectively localized at the contra-lacunar plasma membrane of osteoclasts, and it plays a critical role in bone resorption, because Ae2 total knockout (Ae2−/−) mice demonstrated severe osteopetrosis associated with remarkable morphological changes of osteoclasts (e.g., enlarged osteoclasts with unfolded ruffled border membrane).

Results

Ae2 Immunolabeling Was Selectively Localized to Contra-Lacunar Cell Membrane of Bone-Resorbing Osteoclasts. Mouse osteoclasts displayed distinct Ae2 immunoreactivity corresponding to the contra-lacunar plasma membrane domain (Fig. 1*A*), whereas Ae2−/− mice did not label at this site by immunofluorescence confocal microscopy (Fig. 1*B*). Ae2 immunoreactivity was also found in rat osteoclasts (Fig. 1 *C* and *D*, respectively). In both species, it is apparent that the Ae2 reaction in the osteoclasts is very distinct along the contra-lacunar cell border, whereas it is lacking in the membrane corresponding to the ruffled border. Thus, Ae2 is likely to play a role as the contra-lacunar mechanism for Cl^- entry and HCO_3^- extrusion.

Ae2−/− Mice Exhibited an Abnormal Bone Phenotype of Osteopetrosis. Our findings show that the bone phenotype of these mutants is characterized by osteopetrosis, as evidenced by x-rays of the wild-type and Ae2−/− mouse heads (Fig. 2*A* and *B*). There was an apparent difference in size of the heads and the overall skeletal development is impaired in the Ae2−/− mice with a higher diffuse radio-density than in the wild-type mice ($n = 4$). It is particularly evident that the lower jaw was hypoplastic in the knockout mice, and the degree of development of upper and lower incisors was apparently also impaired. In contrast, the molar teeth had a radio-density comparable to that of the wild-type. The altered bone formation and remodeling in

Author contributions: K.J., J.P., S.F., S.N., and O.F. designed research; K.J., J.P., S.F., and O.F. performed research; L.R.G. contributed new reagents/analytic tools; K.J., J.P., S.F., P.A., S.N., and O.F. analyzed data; and K.J., J.P., T.-H.K., and O.F. wrote the paper.

The authors declare no conflict of interest.

[1]To whom correspondence may be addressed. E-mail: sn@ana.au.dk or pagre@jhsph.edu.

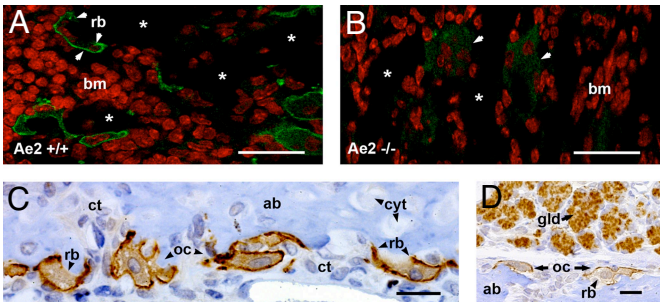

Fig. 1. Immunolocalization of Ae2 in mouse and rat osteoclasts in paraffin sections of decalcified tissue blocks. (*A*) Laser scanning confocal microscopy demonstrated intense immunostaining of the curved contra-lacunar surfaces in osteoclasts from the skull base of Ae2+/+ mice (green fluorescence, arrows). No immunostaining was seen corresponding to the ruffled border (rb). (*B*) Osteoclasts from the same area in knockout mice (Ae2−/−) showed no surface labeling (arrows). Nuclei are shown in red, many of which belong to bone marrow cells (bm). Black background represents bone tissue (asterisks). (*C* and *D*) Rat osteoclasts (oc) attached to alveolar bone (ab) surrounding the maxillary incisor also showed labeling of the contra-lacunar surface domain and unlabeled ruffled borders (rb). cyt, osteocytes; ct, connective tissue of periodontal membrane; gld, glandular tissue of the lateral nasal gland cupping the outer aspect of the alveolar bone also shows immunolocalization of Ae2. Rat, Ae2+/+, and Ae2−/− mouse osteoclasts also displayed a weak cytoplasmic labeling. (Scale bars, 20 μm.)

Ae2−/− mice was also observed in Goldner's trichrome stained paraffin sections of the animals (Fig. 2 *C* and *D*). The bone marrow cavity was occupied by irregular bone speculae in the Ae2−/− mice, and larger cells could be discerned along the speculae. Also, the endochondral ossification zone was widened in Ae2−/− mice.

Osteoclasts in AE2−/− Mice Were Enlarged and Their Ruffled Border Membranes Were Not Folded. In humans, osteoclasts lacking either carbonic anhydrase II (6) or H^+-ATPase (13) also fail to resorb bone, but the osteoclasts look morphologically normal. This is in contrast to the present findings in Ae2−/− mice. In 1-μm–thick toluidine blue-stained sections of epon embedded bone, the irregular bone formation of Ae2−/− mice (Fig. 3*B*) was closely associated with accumulation of large, almost ballooned,

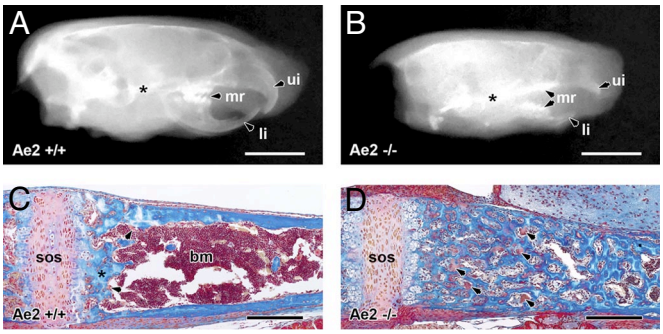

Fig. 2. Ae2-deficient mice develop osteopetrosis. (*A* and *B*) X-ray images of half heads from 15-day-old mice demonstrated an increase in bone density in knockout mice (Ae2−/−) compared with controls (Ae2+/+) especially at the skull base (asterisk). ui, upper incisor; li, lower incisor; mr, molar tooth region. (Scale bars, 5 mm.) (*C* and *D*) Sagittal sections from methyl methacrylate embedded, undecalcified tissue blocks of the base of the skull from Ae2+/+ and Ae2−/− mice stained with Goldner's trichrome. The wide bone marrow cavity (bm) in Ae2+/+ mice filled with hematopoietic cells was in Ae2−/− mice almost obliterated by interwoven endochondral bone trabeculae. sos, cartilage plate of spheno-occipital synchondrosis; arrows, osteoclasts. (Scale bars, 200 μm.)

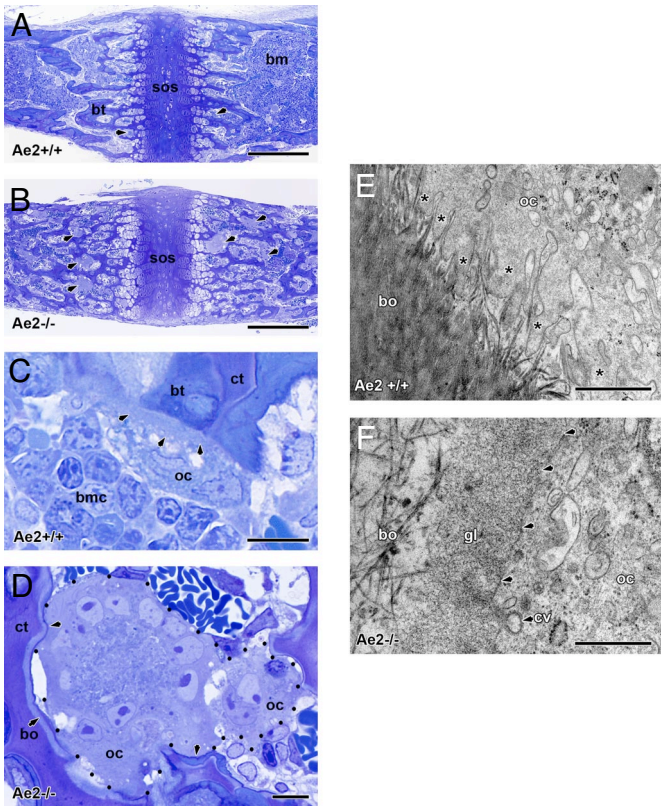

Fig. 3. Epon sections of decalcified bone tissue from the skull base of Ae2+/+ and Ae2−/− mice stained with toluidine blue. Osteoclasts in Ae2−/− mice are morphologically distinct from those of Ae2+/+ mice. (*A*) In Ae2+/+ mice, the endochondral bone formation at the skull base was characterized by a smaller number of bone trabeculae (bt) with narrow remnants of cartilage matrix. Large medullary cavities (bm) with osteoclasts (arrows) were seen on each side of the cartilage plate of the spheno-occipital synchondrosis (sos). (*B*) In Ae2−/− mice, the bone trabeculae were interweaving and contained wide plates of cartilage matrix. The medullary cavity was reduced to narrow compartments occupied by voluminous osteoclasts (arrows). sos, spheno-occipital synchondrosis. (Scale bars, 200 μm.) (*C*) Osteoclasts (oc) from Ae2+/+ mice showed a distinct ruffled border (arrows) apposed to the bone. bt, bone trabecula with cartilage matrix (ct); bmc, bone marrow cells. (*D*) In Ae2−/− mice, osteoclasts (oc, inside dotted boundary line) were expanded in size and did not form distinct ruffled borders (arrows). Trabeculae of cartilage matrix plates (ct) were bordered by a thin layer of bone matrix (bo) having a basophilic surface zone. (Scale bars, 10 μm.) (*E*) Electron micrograph of the resorptive surface area in an osteoclast (oc) from Ae2+/+ mice reveals the complex folding of the resorbing surface into a ruffed border (asterisks) with deep invaginations containing collagen fibrils from the bone matrix (bo). (*F*) In Ae2−/− mice, the cell surface of osteoclasts (oc) apposed to bone (arrows) was smooth without membrane invaginations (arrows) but demonstrated coated endocytosis vesicles (cv). A finely textured granular layer (gl) was present between the osteoclast membrane and a loosely structured collagen matrix of the bone (bo). [Scale bars, 1 μm (*E*) and 500 nm (*F*).]

multinuclear cells compared with osteoclasts of control mice (Fig. 3 *C* and *D*). In the Ae2−/− mice, the cells were very large, and both the cytoplasm and nucleoplasm appear swollen. At the light microscopical level, it is not possible to identify a distinct ruffled border in Ae2−/− mice, whereas the location of such borders appears very distinct in the wild-type osteoclasts. The zone around the ruffled border was further studied by electron microscopy. The normal ruffled border showed a highly irregularly folded cell membrane intimately facing collagen fibers of the bone surface as shown in Fig. 3*E*. Such infolding were not seen in the Ae2−/− mice, and instead, the interface between the cell membrane of the multinuclear cells was a rather smooth (Fig. 3*F*).

Discussion

Osteoclasts are multinucleated bone-resorbing cells responsible for constant bone remodeling. A prerequisite for bone resorption is the ability of osteoclasts to create a closed space between their ruffled border membrane and bone surface. Regulation of pH in the space (i.e., a lacuna) is actively maintained at very low levels, enabling the dissolution of calcium salts from the organic bone matrix. Vacuolar H^+-ATPase and H^+/Cl^- exchanger (ClC-7) localized at the ruffled border membrane of the osteoclasts are known to play a crucial role in establishing low pH of the lacunae (2–4). In contrast, little is known about bicarbonate transport mechanisms in osteoclasts, which also would be important for bone resorption. Intracellular H^+ and HCO_3^- is formed from H_2O and CO_2 catalyzed by carbonic anhydrase II (CA II). H^+ is transported across the ruffled border into the lacunae by a V-ATPase. HCO_3^- may be transported to the contra-lacunar extracellular space by a transporter of unknown molecular identity and possibly coexpress with the carbonic anhydrase XIV, which is located at the contra-lacunar membrane domain of the osteoclasts (14).

In the present study, we demonstrated that the anion exchanger Ae2 is localized at the contra-lacunar membrane of bone-resorbing osteoclasts. This indicates that Ae2 is likely to play a role as the contra-lacunar mechanism for Cl^- entry and HCO_3^- extrusion. The altered function of bone-resorbing osteoclasts in Ae2−/− knockout mice was directly confirmed by the observed severe osteopetrosis, where the skeletal development was impaired with a higher diffuse radio-density on x-ray examination and the bone marrow cavity was occupied by irregular bone speculae. Moreover, Ae2−/− mice exhibited enlarged osteoclasts in size with unfolded ruffled border membranes, in contrast to the normal morphology of these cells in mice lacking either carbonic anhydrase II (6) or H^+-ATPase (15). Kornak *et al.* (4) found that the osteoclasts in ClC-7−/− knockouts only showed rudimentary ruffled border membranes, but no changes in cell volume were reported. The size increase of osteoclasts from Ae2−/− mice was paralleled by a greater number of nuclei in these cells, perhaps suggesting an enlarged nuclear proliferation-cell division ratio. Gawenis *et al.* (11) developed a mouse model carrying a targeted disruption of the Slc4a2 gene to demonstrate the role of Ae2 in gastric acid secretion. Between 10 and 15 days of age, Ae2−/− mice exhibited severe growth retardation, became mildly ataxic, and showed a failure of tooth eruption and defective development of bone. Ae2 exists in three forms because of alternative promoter use, yielding the gene products Ae2a, Ae2b, and Ae2c. Ae2c disruption may be imperative for development of severe calvarial osteopetrosis based on our observations of the total Ae2−/− mouse in this and previous studies. An Ae2a/Ae2b specific knockout mouse model revealed much milder phenotype, in which macroscopic skeletal abnormalities (16) and tooth eruption (17) was much less affected*.

Thus, the molecular mechanisms involved in bone resorption by the osteoclasts mirror tissues in which an anion exchanger match active H^+ extrusion, for example, the parietal cells and renal intercalated cells. Little is known about molecular mechanisms of bicarbonate transport in osteoclasts. It is of interest to study whether other types of HCO_3^- transporters are also expressed in osteoclasts in addition to the Ae2 observed in the present study. A recent study by Bouyer *et al.* (18) showed that a colony-stimulating factor-1 (CSF-1)-induced rise in pH_i in osteoclasts was insensitive to the 4,4′-diisothiocyanatostilbene-2,2′-disulfonic acid (DIDS), whereas it was abolished by removing extracellular sodium. This inhibition profile was similar to that of electroneutral sodium-bicarbonate cotransporter NBCn1 (19). Compatible with this finding, reverse-transcriptase polymerase chain reaction (RT-PCR) revealed the transcripts of an electroneutral NBCn1 in both rat osteoclasts and osteoclast-like cells (18). Immunoblotting also showed the expression of NBCn1 protein in osteoclast-like cells (18), indicating that other type of HCO_3^- transporters (i.e., electroneutral NBCn1) is also present in osteoclasts in addition to the presence of Ae2, and hence, HCO_3^- transport would be important in the regulation of both pH_i and bone resorption. Further studies are needed to define the subcellular localization of HCO_3^- transporters in osteoclasts comprehensively and the role of an altered HCO_3^- transport of osteoclasts in the pathological conditions of bone resorption.

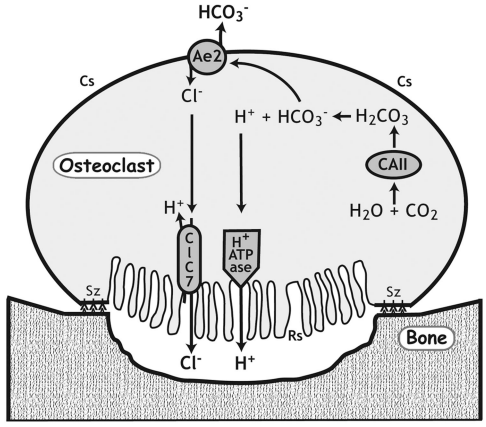

Fig. 4. Diagram of an osteoclast indicating the processes involved in acidification of the resorptive lacuna. The osteoclast is attached on bone with a tight circumferential sealing zone (Sz) that divides the cell surface into two separate domains, the resorptive surface (Rs), folded into a ruffled border within the sealing zone, and the contra-lacunar surface (Cs). Intracellular H^+ and HCO_3^- are formed from H_2O and CO_2 catalyzed by carbonic anhydrase II (CA II). H^+ is transported across the ruffled border into the resorption lacuna by a vacuolar-type H^+-ATPase. Cl^- ions follow H^+ to the lacunae through the H^+/Cl^- exchangers (ClC-7) and maintain electroneutrality. Excess HCO_3^- would, in time, cause cytoplasmic alkalinization and is removed via a contra-lacunar Cl^-/HCO_3^- exchange by Ae2, which also provides the cells with Cl^- for secretion into the lacunar space.

In summary, we demonstrated that that Ae2 is expressed in contra-lacunar membranes of osteoclasts of mice and rats. Ae2 expression in osteoclasts seems essential for normal bone formation and resorption, because genetic disruption of Ae2 led to osteopetrosis. Although osteopetrosis is also seen in mice with genetic disruption of the ClC-7 exchanger, H^+-ATPase, and carbonic anhydrase II (4, 15, 20), the substantial changes in the morphology of the osteoclasts seem specific for Ae2 deficiency. The identification of Ae2 as the contra-lacunar mediator of basolateral Cl^- uptake and HCO_3^- extrusion suggests an updated model of the set of molecular mechanisms involved in lacunar acidification (Fig. 4) and the potential role of HCO_3^- transport in osteoclasts in the pathophysiology of altered bone resorption.

Materials and Methods

Animals. Development of the mouse model carrying a targeted disruption of the Ae2 (Slc4a2) gene has been described in detail (11). Four homozygous null mutants (Ae2−/−) mice and four gender-matched wild-type (Ae2+/+) littermates, all aging 15 to 16 days, were perfusion fixed via the left ventricle with 4% paraformaldehyde in isotonic phosphate buffered salt solution (PBS, pH 7.4) and post-fixed. Male Wistar rats, weighing 100 g, were perfusion fixed with 4% paraformaldehyde in 0.1 M sodium cacodylate buffer (pH 7.4). The jaws were dissected and left overnight in the same fixative.

*Osteoclast function was less affected in the calvarium than in long bone of Ae2a/Ae2b specific knockout mice. [Jansen I, De Vries T, Ravesloot J, Everts V, Oude Elferink R. (2006) Loss of anion exchanger 2 (Ae2) in mice results in osteopetrosis. *J Bone Miner Res* 21:S68 (abstr).]

Immunolabeling and Laser Scanning Confocal Microscopy. A previously characterized rabbit polyclonal antibody recognizing the Ae2a and Ae2b isoforms was used (12). Decalcified bone tissue (see below) from the skull base was embedded in paraffin, and 2-μm sections immunolabeled as described in the same study by using Alexa488 conjugated goat anti-rabbit secondary antibody (Invitrogen) to visualize the primary antibody and To-Pro-3 (Invitrogen) for visualization of cell nuclei. Images were acquired on an inverted Leica DMRS confocal microscope by using an HCX PlApo 64$\times$ (1.32 NA) objective (21). For peroxidase staining, the secondary antibody was horseradish peroxidase-conjugated goat anti-rabbit IgG (Dako), and 0.05% 3,3′diaminobenzidine tetrahydrochloride was used for visualization. Mayer's hematoxylin was used for counterstaining, and microscopy was performed on a Leica DMRE bright-field microscope equipped with a Leica DM300 digital camera.

X-Ray Analysis. Mouse heads were divided midsagittally and radiographed by using an GX-1000 x-ray unit (Gendex) with circular collimation at 50 kVp, 10 mA, and a 45-cm focus-receptor distance. Digital x-ray images were obtained with a Dixi CCD-based sensor system (Planmeca) at an exposure time of 0.42 s and transferred to Adobe Photoshop (Adobe Systems) for adjustment of magnification.

Light Microscopy. Mouse heads, bone tissue dissected from the mouse skull base, and rat jaws were decalcified in 4.13% EDTA (pH 7.4) at 4°C for 6 and 20 days, respectively and subsequently washed in 0.1 M sodium cacodylate buffer (pH 7.4). Decalcified and undecalcified specimens were then processed for embedding in paraffin or methyl methacrylate (MMA) (Merck) using standard procedures. Two-micrometer-thick sagittally oriented serial sections were cut from MMA- and paraffin-embedded blocks and stained with Goldner's trichrome or prepared for immunohistochemistry, respectively. Sections were photographed with a Nikon D1 camera attached to an Olympus BH2 microscope.

Electron Microscopy. Decalcified bone tissue from the skull base was immersion fixed in 4% paraformaldehyde in 0.1 M sodium cacodylate buffer containing 1% glutaraldehyde (pH 7.2) for 1 d at 4°C. This was followed by postfixation in 1% osmium tetraoxid for 2 h at 4°C. After rinsing, the tissue was dehydrated in a series of alcohol, transferred to propylenoxide, and embedded in EPON. Semithin sections (0.5–1 μm) were mounted on glass slides and stained with toluidine blue. Ultrathin sections were prepared by using a Reichert ultramicrotome, mounted on 200 mesh nickel grids, and stained with uranyl acetate and lead. Images were recorded in a FEI-Morgagni microscope operating at 80 kV by using a CCD camera (MegaViewIII, SIS).

ACKNOWLEDGMENTS. The authors thank Inger Merete Paulsen, Jette Barlach, and Helle Høyer for expert technical assistance. The Water and Salt Research Centre at the University of Aarhus is established and supported by the Danish National Research Foundation (Danmarks Grundforskningsfond). Support for this study was also obtained from The Danish Medical Research Council and Korea Science and Engineering Foundation Grant R01–2007-000–20441–0, funded by the Ministry of Education, Science, and Technology.

1. Tolar J, Teitelbaum SL, Orchard PJ (2004) Osteopetrosis. *N Engl J Med* 351:2839–2849.
2. Blair HC, Teitelbaum SL, Ghiselli R, Gluck S (1989) Osteoclastic bone resorption by a polarized vacuolar proton pump. *Science* 245:855–857.
3. Vaananen HK, *et al.* (1990) Evidence for the presence of a proton pump of the vacuolar H(+)-ATPase type in the ruffled borders of osteoclasts. *J Cell Biol* 111:1305–1311.
4. Kornak U, *et al.* (2001) Loss of the ClC-7 chloride channel leads to osteopetrosis in mice and man. *Cell* 104:205–215.
5. Silver IA, Murrills RJ, Etherington DJ (1988) Microelectrode studies on the acid microenvironment beneath adherent macrophages and osteoclasts. *Exp Cell Res* 175:266–276.
6. Sly WS, Hewett-Emmett D, Whyte MP, Yu YS, Tashian RE (1983) Carbonic anhydrase II deficiency identified as the primary defect in the autosomal recessive syndrome of osteopetrosis with renal tubular acidosis and cerebral calcification. *Proc Natl Acad Sci USA* 80:2752–2756.
7. Teti A, *et al.* (1989) Cytoplasmic pH regulation and chloride/bicarbonate exchange in avian osteoclasts. *J Clin Invest* 83:227–233.
8. Alper SL (2006) Molecular physiology of SLC4 anion exchangers. *Exp Physiol* 91:153–161.
9. Ribeiro ML, *et al.* (2000) Severe hereditary spherocytosis and distal renal tubular acidosis associated with the total absence of band 3. *Blood* 96:1602–1604.
10. Sander T, *et al.* (2002) Association of the 867Asp variant of the human anion exchanger 3 gene with common subtypes of idiopathic generalized epilepsy. *Epilepsy Res* 51:249–255.
11. Gawenis LR, *et al.* (2004) Mice with a targeted disruption of the AE2 Cl^-/HCO_3^- exchanger are achlorhydric. *J Biol Chem* 279:30531–30539.
12. Frische S, *et al.* (2004) AE2 isoforms in rat kidney: Immunohistochemical localization and regulation in response to chronic NH_4Cl loading. *Am J Physiol Renal Physiol* 286:F1163–F1170.
13. Frattini A, *et al.* (2000) Defects in TCIRG1 subunit of the vacuolar proton pump are responsible for a subset of human autosomal recessive osteopetrosis. *Nat Genet* 25:343–346.
14. Riihonen R, *et al.* (2007) Membrane-bound carbonic anhydrases in osteoclasts. *Bone* 40:1021–1031.
15. Li YP, Chen W, Liang Y, Li E, Stashenko P (1999) Atp6i-deficient mice exhibit severe osteopetrosis due to loss of osteoclast-mediated extracellular acidification. *Nat Genet* 23:447–451.
16. Medina JF, *et al.* (2003) Anion exchanger 2 is essential for spermiogenesis in mice. *Proc Natl Acad Sci USA* 100:15847–15852.
17. Lyaruu DM, *et al.* (2008) The anion exchanger Ae2 is required for enamel maturation in mouse teeth. *Matrix Biol* 27:119–127.
18. Bouyer P, *et al.* (2007) Colony-stimulating factor-1 increases osteoclast intracellular pH and promotes survival via the electroneutral Na/HCO3 cotransporter NBCn1. *Endocrinology* 148:831–840.
19. Choi I, Aalkjaer C, Boulpaep EL, Boron WF (2000) An electroneutral sodium/bicarbonate cotransporter NBCn1 and associated sodium channel. *Nature* 405:571–575.
20. Margolis DS, Szivek JA, Lai LW, Lien YH (2008) Phenotypic Characteristics of Bone in Carbonic Anhydrase II-Deficient Mice. *Calcif Tissue Int* 82:66–76.
21. Damkier HH, Nielsen S, Praetorius J (2007) Molecular expression of SLC4-derived Na^+-dependent anion transporters in selected human tissues. *Am J Physiol Regul Integr Comp Physiol* 293:R2136–R2146.